



This is a repository copy of *OPG-Fc inhibits ovariectomy-induced growth of disseminated breast cancer cells in bone*.

White Rose Research Online URL for this paper:  
<http://eprints.whiterose.ac.uk/90511/>

Version: Accepted Version

---

**Article:**

Ottewell, P.D., Wang, N., Brown, H.K. et al. (4 more authors) (2015) OPG-Fc inhibits ovariectomy-induced growth of disseminated breast cancer cells in bone. *International Journal of Cancer*, 137 (4). 968 - 977. ISSN 0020-7136

<https://doi.org/10.1002/ijc.29439>

---

This is the peer reviewed version of the following article: Ottewell, P. D., Wang, N., Brown, H. K., Fowles, C. A., Croucher, P. I., Eaton, C. L. and Holen, I. (2015), OPG-Fc inhibits ovariectomy-induced growth of disseminated breast cancer cells in bone. *Int. J. Cancer*, 137: 968–977, which has been published in final form at <http://dx.doi.org/10.1002/ijc.29439>. This article may be used for non-commercial purposes in accordance with Wiley Terms and Conditions for Self-Archiving

**Reuse**

Unless indicated otherwise, fulltext items are protected by copyright with all rights reserved. The copyright exception in section 29 of the Copyright, Designs and Patents Act 1988 allows the making of a single copy solely for the purpose of non-commercial research or private study within the limits of fair dealing. The publisher or other rights-holder may allow further reproduction and re-use of this version - refer to the White Rose Research Online record for this item. Where records identify the publisher as the copyright holder, users can verify any specific terms of use on the publisher's website.

**Takedown**

If you consider content in White Rose Research Online to be in breach of UK law, please notify us by emailing [eprints@whiterose.ac.uk](mailto:eprints@whiterose.ac.uk) including the URL of the record and the reason for the withdrawal request.



[eprints@whiterose.ac.uk](mailto:eprints@whiterose.ac.uk)  
<https://eprints.whiterose.ac.uk/>



**OPG-Fc inhibits ovariectomy-induced growth of disseminated breast cancer cells in bone**

Journal:	<i>International Journal of Cancer</i>
Manuscript ID:	IJC-14-2560.R1
Wiley - Manuscript type:	Cancer Therapy
Date Submitted by the Author:	n/a
Complete List of Authors:	Ottewell, Penelope; University of Sheffield, Oncology Wang, Ning; University of Sheffield, Human Metabolism Brown, Hannah; University of Sheffield, Human Metabolism Fowles, Anne; University of Sheffield, Human Metabolism Croucher, Peter; Garvan Institute of Medical Research, Musculoskeletal Medicine Eaton, Colby; University of Sheffield, Human Metabolism Holen, Ingunn; University of Sheffield, Oncology
Key Words:	Breast cancer, Metastasis, Bone, OPG-Fc

SCHOLARONE™  
Manuscripts

1  
2  
3 **OPG-Fc inhibits ovariectomy-induced growth of disseminated breast**  
4 **cancer cells in bone**  
5  
6

7  
8 Penelope D Ottewell<sup>1</sup>, Ning Wang<sup>2</sup>, Hannah K Brown<sup>1</sup>, C Anne Fowles<sup>2</sup>, Peter I Croucher<sup>3</sup>,  
9 Colby L Eaton<sup>2</sup> and Ingunn Holen<sup>1</sup>  
10

11  
12  
13  
14 <sup>1</sup>Academic Unit of Clinical Oncology, Department of Oncology, <sup>2</sup> Academic Unit of Bone  
15 Biology, Department of Human Metabolism, University of Sheffield, S10 2RX, UK and  
16  
17 <sup>3</sup>Musculoskeletal Medicine Division, Garvan Institute of medical Research, Sidney, New  
18 South Wales, Australia.  
19  
20

21  
22  
23  
24 **Corresponding author:** Dr. Penelope Ottewell, Academic Unit of Clinical Oncology, Medical  
25 School, University of Sheffield, Beech Hill Road, Sheffield, S10 2RX, UK.  
26

27  
28 Telephone: +44 (0) 114 271 2133  
29

30 Fax: +44 (0) 114 271 1711  
31

32  
33 E-Mail : [p.d.ottewell@sheffield.ac.uk](mailto:p.d.ottewell@sheffield.ac.uk)  
34  
35  
36  
37

38 **Key Words :** Breast Cancer, OPG, Metastasis, Bone  
39

40 **Short title :** OPG-Fc inhibits breast cancer bone metastasis  
41  
42  
43  
44  
45  
46  
47  
48  
49  
50  
51  
52  
53  
54  
55  
56  
57  
58  
59  
60

**Abstract**

**Background:** Dormant disseminated tumour cells can be detected in the bone marrow of breast cancer patients several years after resection of the primary tumour. The majority of these patients will remain asymptomatic, however, ~15% will go on to develop overt bone metastases and this condition is currently incurable. The reason why these dormant cells are stimulated to proliferate and form bone tumours in some patients and not others remains to be elucidated. We have recently shown that in an *in vivo* model, increasing bone turnover by ovariectomy stimulated proliferation of disseminated tumour cells, resulting in formation of bone metastasis. We now show for the first time that osteoclast mediated mechanisms induce growth of tumours from dormant MDA-MB-231 cells disseminated in the bone. We also show that disruption of RANK-RANKL interactions following administration of OPG-Fc inhibits growth of these dormant tumour cells *in vivo*. Our data support early intervention with anti-resorptive therapy in a low-oestrogen environment to prevent development of bone metastases.

## Introduction

Metastatic breast cancer remains a considerable clinical challenge, causing around 12,000 deaths annually in the UK alone. The majority of patients with advanced disease will develop bone metastases, in many cases several years after removal of the primary tumour. It is increasingly accepted that, in breast cancer, the dissemination of tumour cells from the primary site to specific niches in the bone marrow is an early event, completed prior to diagnosis and initiation of therapy. Tumour cells can remain dormant in the bone marrow for decades and may never proliferate to form overt bone metastases. The precise cellular and molecular mechanisms that regulate tumour cell dormancy in bone, and the signals that trigger tumour cell escape from dormancy, remain to be established. However, the tumour microenvironment is suggested to play a major role in both processes, and therefore represents a key therapeutic target (1-2).

Development and progression of breast cancer bone metastases has been intensely studied, demonstrating that the process is driven by close interactions between tumour cells and components of the bone microenvironment. In particular, tumour cell-mediated stimulation of the bone-resorbing osteoclasts is shown to be responsible for the lytic bone lesions associated with late stage disease (3). In contrast, our understanding of the early stages of tumour cell dissemination to the skeleton, as well as the initiation of tumour cell growth, is less clearly defined. Both osteoblasts and osteoclasts, as well as components of the extracellular matrix, are proposed to play a role in the early stages of bone metastasis (reviewed in: 3,4).

Due to the key role of the bone microenvironment, treatment of overt bone metastases involves a combination of agents that target tumour cells directly as well as bone-targeted agents like bisphosphonates and denosumab (5,6). However, whether adjuvant targeting of the bone microenvironment (in particular the osteoclast) can reduce bone metastasis remains controversial. The recently published AZURE trial found that treating breast cancer patients considered at high risk of developing bone metastases with Zoledronic acid was only beneficial in patients with established menopause (7). This surprising result has been confirmed in other clinical trials, but the underlying mechanisms are yet to be identified. Adjuvant trials of denosumab are ongoing (D-CARE), and will provide further information as to whether osteoclast-mediated processes are key to the differential effects on breast cancer bone metastasis according to menopausal status.

1  
2  
3 One of the main unanswered questions in relation to initiation of bone metastasis is  
4 how changes to the bone microenvironment, including accelerated bone turnover, affects  
5 disseminated tumour cells in bone. Recent advances in technology have facilitated the  
6 studies of individual tumour cells within their resident bone niches. We and others have  
7 used a combination of *in vivo* bone metastasis models and advanced imaging to investigate  
8 how bone-targeted agents modify the bone microenvironment and how this affects  
9 subsequent tumour cell homing/proliferation (8-12,). Using this approach, we recently  
10 demonstrated that accelerated bone turnover caused by ovariectomy (OVX) resulted in  
11 proliferation of disseminated tumour cells and increased levels of bone metastases (8).  
12 Tumour growth in bone was inhibited by the anti-resorptive agent zoledronic acid,  
13 suggesting that osteoclast activity is involved in regulating early stages of bone metastasis,  
14 as well as in end stage disease. If this hypothesis is correct, other anti-resorptive agents  
15 working through different mechanisms should also prevent both OVX-induced bone loss and  
16 growth of dormant tumour cells in bone. The agent of choice to investigate this is  
17 denosumab, a monoclonal antibody that binds human receptor activator of nuclear factor  
18 (NF)- $\kappa$ B ligand (RANKL) with high affinity, thereby blocking RANK-RANKL interactions  
19 essential for osteoclastogenesis. Denosumab is shown to be superior to zoledronic acid for  
20 the prevention or delay of skeletal complications in patients with advanced cancer and bone  
21 metastases (13). However, denosumab is human specific and cannot be used in murine *in*  
22 *vivo* models. Instead we have used OPG-Fc, a potent inhibitor osteoclastogenesis that acts  
23 by preventing RANKL-RANK binding and hence modifies the same pathways as denosumab  
24 (14). We investigated the effects of inhibiting OVX-induced bone resorption through  
25 targeting RANKL-RANK interactions in an *in vivo* model of disseminated breast cancer cells in  
26 bone.  
27  
28  
29  
30  
31  
32  
33  
34  
35  
36  
37  
38  
39  
40  
41  
42

43 The current study is the first to demonstrate that administration of OPG-Fc inhibits  
44 OVX-induced growth of disseminated, dormant, tumour cells in bone *in vivo*. Our data  
45 support the early administration of anti-resorptive therapy in a low-oestrogen setting to  
46 prevent development of bone metastases.  
47  
48  
49  
50  
51  
52  
53  
54  
55  
56  
57  
58  
59  
60

## Materials and methods

**Cell Culture:** Low passage (< P10) human MDA-MB-231 breast cancer cells transfected with the red fluorescent protein, TdTomato (RFP) and second generation luciferase (luc-2) (Calliper Life Sciences, Manchester, UK) were cultured in DMEM + 10% FCS (Gibco®, Invitrogen, Paisley, UK). Prior to injection, tumour cells were incubated for 15 minutes with 25µM of 1,1'-Dioctadecyl-, 3'-Tetramethylindodicarbocyanine, 4-Chlorobenzenesulfonate (DiD) (Life Technologies, Paisley, UK). DiD is a lipophilic membrane dye that becomes diluted each time the cell divides enabling visualisation of non-proliferating, disseminated tumour cells in bone by 2-photon microscopy. Tumour growth was monitored using an IVIS Lumina II system (Calliper Life Sciences).

**In vitro experiments:** For cell proliferation experiments,  $1 \times 10^4$  MDA-MB-231 cells were seeded in 2mls of DMEM + 0, 2.5, 5, 7.5 or 10% FCS in 12 well tissue culture plates (Corning, Paisley, UK). 24h after seeding cells were treated with 0, 10, 50 or 100µg/ml recombinant OPG (OPG-Fc) (comprising amino acids 22-194 of human OPG fused at the N-terminus of the Fc domain of human immunoglobulin G1 (15)). This compound is certified as endotoxin free and was a kind gift from Amgen). Cells were harvested using trypsin/EDTA (SigmaAldrich, Poole, UK) at 24, 48, 72 and 144h and numbers of tumour cells were counted using a hemacytometer. For clonogenic assays 1000 or 500 cells were seeded into 6-well tissue culture plates containing saline / 100µg/ml OPG-Fc in 2mls DMEM or into 2mls of DMEM and left for 24h before addition of OPG-Fc. All experiments were carried out three times in triplicate

**In vivo studies:** We used 12-week-old female BALB/c nude mice (Charles River, Kent, UK). Experiments were carried out in accordance with local guidelines and with Home Office approval under project licence 40/3462, University of Sheffield, UK.

To investigate the effects of ovariectomy on dormant tumour cells in bone,  $1 \times 10^5$  MDA-MB-231 cells were injected into the left cardiac ventricle of 19 mice. Mice were ovariectomised or sham ovariectomised (n=7/group) 56 days after tumour cell injection and culled 28 days

1  
2  
3 later. In addition, 5 mice were culled on day 56 and analysed for presence of disseminated  
4 tumour cells in the long bones.  
5

6  
7 Effects of OPG-Fc on bones were analysed 4 weeks following weekly intra-venous injection  
8 (i.v) of 25mg/kg OPG-Fc. Effects of OPG-Fc on ovariectomy-induced tumour growth were  
9 investigated in mice injected into the left cardiac ventricle with  $1 \times 10^5$  DiD labelled MDA-MB-  
10 231 cells on day 0. On day 5 mice were given weekly OPG-Fc (25mg/kg i.v) or saline  
11 (n=20/group) and on day 7, animals from both groups underwent either sham or  
12 ovariectomy (n=7/group).  
13  
14  
15

16  
17 Whole blood was collected by cardiac puncture and the isolated serum was stored at  $-80^{\circ}\text{C}$   
18 for ELISA, tibiae and femurs were fixed in 4% PFA for  $\mu\text{CT}$  analysis before decalcification in  
19 1%PFA/0.5% EDTA and processing for histology. Bones for two-photon analysis were stored  
20 in OCT at  $-80^{\circ}\text{C}$ .  
21  
22  
23  
24

25  
26  
27 **Microcomputed tomography imaging:** Microcomputed tomography analysis was carried out  
28 using a Skyscan 1172 x-ray-computed microtomography scanner (Skyscan, Aartselaar,  
29 Belgium) equipped with an x-ray tube (voltage, 49kV; current, 200uA) and a 0.5-mm  
30 aluminium filter was used. Pixel size was set to  $5.86 \mu\text{m}$  and scanning initiated from the top  
31 of the proximal tibia as previously described (16).  
32  
33  
34  
35  
36  
37

38  
39 **Bone histology:** Histological sections ( $5 \mu\text{M}$ ) of decalcified tibiae ( $5 \mu\text{mol/L}$  EDTA for 4 weeks)  
40 were stained with Goldner's trichrome or Safranin O using standard protocols. Osteoclasts  
41 were detected by tartrate-resistant acid phosphatase (TRAP) staining and osteoblasts were  
42 identified as mononuclear, cuboidal cells residing in chains along the bone surface as  
43 previously described (17).  
44  
45  
46  
47  
48  
49

50 **Two-photon microscopy:** Detection of individual tumour cells disseminated into mouse  
51 tibiae in which no tumour growth was observed by luciferase imaging was carried out by  
52 two-photon microscopy. Dissected tibias were snap frozen in liquid nitrogen, embedded in  
53 CryoMBed embedding medium and trimmed longitudinally to expose bone marrow area  
54 using a cryostat (Bright 126 Instrument Co. Ltd). A stack area of  $2104 \mu\text{m}$  (X) x  $2525 \mu\text{m}$  (Y) x  
55  
56  
57  
58  
59  
60



1  
2  
3 100µm (Z) incorporating the proximal tibiae was imaged (Zeiss LSM510 NLO microscope Carl  
4 Zeiss Inc). DiD labelled, non-proliferating, tumour cells were visualised using a 633nm  
5 Chameleon laser, bone was detected using the 900nm multiphoton laser (Coherent, Santa  
6 Clara, CA.) and images were reconstructed in LSM software version 4.2 (Zeiss).  
7  
8

9  
10  
11  
12 **Biochemical analysis:** Serum concentrations of TRAP 5b and P1NP were measured using  
13 commercially available ELISA kits: MouseTRAP™ Assay (Immunodiagnostic systems) and  
14 Rat/Mouse P1NP competitive immunoassay kit (Immunodiagnostic Systems), respectively.  
15  
16

17  
18  
19  
20 **Statistical Analysis:** Statistical analysis was by one way analysis of variance (ANOVA)  
21 followed by Newman-Keuls multiple comparison test. Statistical significance was defined as  
22 P less than or equal to 0.01. All P values are two-sided.  
23  
24  
25  
26  
27  
28  
29  
30  
31  
32  
33  
34  
35  
36  
37  
38  
39  
40  
41  
42  
43  
44  
45  
46  
47  
48  
49  
50  
51  
52  
53  
54  
55  
56  
57  
58  
59  
60

## Results

### Effects of ovariectomy on growth of dormant breast cancer cells in bone

We have previously shown that ovariectomy (OVX) increases bone turnover in 12-week old mice and that performing OVX, either 7 days before or 7 days after intra-cardiac (i.c.) injection of breast cancer cells, results in significantly increased bone metastasis (8). To more closely mimic the clinical situation, where disseminated tumour cells lie dormant in bone for prolonged periods, we have now investigated whether OVX also induces growth of tumour cells that have remained non-proliferative in bone for 8 weeks. BALB/c nude mice were injected i.c. with MDA-MB-231 cells on day 0 and monitored by weekly *in vivo* imaging. If animals had not developed long bone metastases by day 56, the disseminated tumour cells in bone were considered to be dormant. Animals without long bone tumours underwent either OVX (n=7) or sham operation (n=7) on day 56. A cohort of animals was culled to confirm the presence of dormant disseminated tumour cells in long bones (n=5) (figure 1a).

As expected, OVX stimulated tumour growth in the long bones, with bone metastases detected in 6/7 mice 4 weeks later (figure 1b). In contrast, no metastases were seen in the long bones of sham operated animals. Tumour growth at other sites, including spine, ribs and head, were comparable in both experimental groups and was unaltered by ovariectomy (figure 1c). Analysis of tibiae 56 days following tumour cell injection confirmed the presence of non-proliferating (dormant) DiD-labelled cells in close proximity to trabecular bone (figure 1d). DiD-labelled tumour cells were detected in the tibia of all mice, including those that did not develop tumours by the end of the experimental protocol (day 84).  **$\mu$ CT analysis of proximal tibiae from OVX and sham operated mice confirmed that OVX significantly reduced trabecular bone volume compared with tissue volume P <0.01 (figure 1 e).**

These data demonstrate that tumour cells can remain dormant in bone for prolonged periods of time *in vivo*, and that altering the bone microenvironment through OVX triggers their proliferation and development into overt bone metastases.

### Effects of OPG-Fc on the bone microenvironment

1  
2  
3 We next investigated whether the OVX-induced changes to the bone microenvironment  
4 could be counteracted by inhibition of bone turnover. Osteoprotegerin (OPG) inhibits  
5 osteoclastogenesis through disrupting RANKL-RANK interactions (14). We established the  
6 effects of weekly administration of 25mg/kg OPG-Fc on the bone microenvironment in our  
7 model system. As shown in figure 2, animals receiving OPG-Fc displayed increased bone  
8 volume, had an extended growth plate and reduced serum levels of markers of both  
9 osteoclast (TRAP) and osteoblast (P1NP) activity, compared to the control group. This was  
10 accompanied by striking reductions in the numbers of osteoblasts and osteoclasts (figure 2a).  
11 Scoring of histological sections revealed  $3.22 \pm 1.46$  osteoclasts and  $98.16 \pm 17.42$   
12 osteoblasts per mm of bone surface in tibiae of control mice, whereas both cell types were  
13 undetectable on endocortical and trabecular surfaces of tibiae 4 weeks following weekly  
14 injection of 25mg/kg OPG-Fc. The most dramatic change was seen in the bone volume, with  
15 the percentage of bone volume compared with tissue volume increasing from  $8.19 \pm 0.29\%$   
16 in control animals to  $23.55 \pm 0.21\%$  in animals receiving OPG-Fc,  $p < 0.001$ . This change was  
17 mainly due to the extended growth plate and increased proteoglycan rich matrix in the  
18 metaphysis of bones from OPG-Fc treated compared with control mice (figure 2a). The  
19 increase in bone volume may, therefore, be a result of elevated ossification due OPG-Fc  
20 induced disruption of osteoclast activity preventing resorption of this access matrix.  
21  
22  
23  
24  
25  
26  
27  
28  
29  
30  
31  
32  
33  
34  
35

### 36 OPG-Fc inhibits OVX-induced growth of disseminated tumour cells

37 Having established that OPG-Fc has no direct effects on the ability of MDA-MB-231 cells to  
38 form colonies or proliferate *in vitro* (Figure 3) we investigated its effects on growth of  
39 disseminated, dormant, tumour cells in the long bones. MDA-MB-231 cells were injected i.c.  
40 in 12-week old BALB/c nude mice that were treated once weekly with either saline (n=14) or  
41 25mg/kg OPG-Fc (n=14) from day 4. Half of the animals in each group underwent either OVX  
42 or a sham operation on day 7 (see outline in Figure 4a). As expected, 78.5% of the animals in  
43 the OVX/saline group developed long bone tumours by day 35, compared to only 14.5% of  
44 the animals in the sham/saline group (Figure 4b,c). Administration of OPG-Fc completely  
45 prevented OVX-induced tumour growth, with 7% animals in the OVX/OPG-Fc group having  
46 detectable long bone tumours, compared to 78.5% in the OVX/saline group. Tumour  
47 frequency in sham-operated animals was unaffected by OPG-Fc (7.5% of animals having  
48 detectable bone metastases in sham/OPG-Fc vs 14.5% in sham/saline). In addition, in the  
49 small number of animals in which tumours did grow in the bone OPG-Fc significantly  
50  
51  
52  
53  
54  
55  
56  
57  
58  
59  
60

1  
2  
3 reduced tumour size in both OVX ( $P < 0.01$ ) and sham OVX ( $P < 0.01$ ) operated mice.  
4  
5 Luciferase imaging showed no effect of OPG-Fc on tumour grown outside of bone (figure 4d)  
6  
7 This is the first demonstration that administration of OPG-Fc has profound inhibitory effects  
8  
9 on disseminated tumour cells *in vivo*, preventing development of overt bone metastases.

### 10 11 12 13 **OPG-Fc prevents OVX-induced changes to the bone microenvironment**

14  
15  
16 In order to confirm that administration of OPG-Fc reversed OVX-induced bone loss, we  
17 carried out a detailed characterisation of the tibia of the animals in the tumour study  
18 described in the previous section. As shown in figure 5 a and b, OPG-Fc caused a highly  
19 significant increase in bone volume compared to saline control in both the OVX and sham  
20 group (percentage of bone volume compared with tissue volume is  $11.49 \pm 0.51\%$  in saline  
21 treated sham operated mice compared with  $24.73 \pm 1.64\%$  in OPG-Fc treated sham mice  
22 ( $P < 0.001$ ) and  $7.86 \pm 0.44\%$  in saline treated OVX mice compared with  $23.98 \pm 3.22\%$  in OPG-  
23 Fc treated OVX mice ( $P < 0.001$ )). The increased bone volume was accompanied by a  
24 corresponding decrease in serum TRAP and P1NP levels ( $P < 0.001$  for sham saline vs. sham  
25 OPG-Fc and  $P < 0.001$  for OVX saline vs. OPG-Fc for both TRAP and P1NP) (figure 5 c and d),  
26 confirming that OPG-Fc counteracts OVX-induced bone loss in the animals where growth of  
27 disseminated tumour cells was inhibited.  
28  
29  
30  
31  
32  
33  
34  
35  
36  
37  
38

### 39 **Discussion**

40  
41 In the current study we have used mouse models of MDA-MB-231 breast cancer cell  
42 dormancy in bone and advanced *in vivo* imaging to investigate the effects of OVX induced  
43 stimulation of osteoclastic bone resorption on the formation of metastases. In addition, we  
44 have studied the effects of targeting RANKL-RANK interactions with OPG-Fc on the  
45 formation and progression of OVX-induced bone metastases.  
46  
47  
48

49  
50 We have previously reported that OVX performed 7 days after tumour cell injection of MDA-  
51 MB-231 breast cancer cells (i.c) leads to increased bone metastases in 12-week old balb/c  
52 mice (8). This result was confirmed in the current study (figure 4). However, our previous  
53 studies did not investigate whether this model reflected the clinical situation, in which bone  
54 metastases are thought to form from dormant tumour cells. In breast cancer patients it is  
55 generally accepted that tumour cells are disseminated in the bone marrow in the early  
56  
57  
58  
59  
60

1  
2  
3 stages of disease, often before diagnosis, and that these cells remain dormant unless  
4 triggered to proliferate as a result of changes in their microenvironment (4-5). In the current  
5 study we show that once MDA-MB-231 tumour cells are disseminated in the bones of 12-  
6 week old Balb/c mice (with low bone turnover) these tumour cells remain dormant in this  
7 environment for the entire 12-week experimental protocol, confirming that our model  
8 mimics tumour cell dormancy. A decrease in circulating oestrogen following OVX leads to  
9 changes in the bone microenvironment in both humans and animal models (18-20), These  
10 changes have the net effect of increasing osteoclastic bone resorption (18-20). Our data  
11 confirm significant bone loss in mice following OVX. Importantly we also show that altering  
12 the bone microenvironment by OVX stimulates proliferation of tumour cells that have  
13 previously been dormant in the bone microenvironment for 8 weeks. OVX stimulation of  
14 dormant tumour cells was specific to long bones and no effects were seen in other bones or  
15 soft tissues. MDA-MB-231 cells primarily home to long bones following i.c. injection in mice  
16 (21) and tumour growth at other sites is uncommon. We therefore hypothesise that lack of  
17 detectable tumour growth by luciferase imaging in bones other than long bones following  
18 OVX may be due to tumour cells not being disseminated in these sites, this may also be true  
19 for lack of tumour growth in soft tissues observed in this model. In the current study only  
20 tibiae were harvested for two-photon analysis of disseminated tumour cells and therefore,  
21 dissemination at other sites remains to be confirmed. MDA-MB-231 breast cancer cells are  
22 oestrogen-independent, whereas the majority of bone metastases occur from oestrogen  
23 receptor positive tumours. In an attempt to better reflect bone metastasis from human  
24 breast cancer, we carried out pilot studies of tumour cell dormancy in bone using oestrogen-  
25 dependent MCF7 cells. In the absence of oestrogen supplementation, these cells did not  
26 form bone metastasis following i.c. injection over the subsequent 20 weeks (data not  
27 shown). In addition, oestrogen supplementation caused major changes to the bone  
28 environment and could not be used in conjunction with OVX (8). We have, therefore,  
29 focused this study on oestrogen-independent cells.

30  
31  
32  
33  
34  
35  
36  
37  
38  
39  
40  
41  
42  
43  
44  
45  
46  
47 Our previous data support that stimulation of disseminated tumour cells in bone to  
48 proliferate and form metastases is likely to be driven by osteoclast-mediated mechanisms  
49 (8). We have now tested this hypothesis by investigating the effects of inhibiting  
50 RANK/RANKL interactions on OVX-induced bone metastases. The binding of RANKL to its  
51 cognate receptor RANK is essential for osteoclast maturation, function and survival. The  
52 presence of tumour cells in the bone environment stimulates production of RANKL from  
53 osteoblasts: *In vitro* co-culture of MDA-MB-231 cells with the human osteoblast cell line  
54  
55  
56  
57  
58  
59  
60

1  
2  
3 MG-63 results in enhanced production of RANKL (22). Furthermore, MDA-MB-231 cells that  
4 do not express RANKL when cultured alone, demonstrate increased RANKL mRNA expression  
5 when co-cultured with primary osteoblasts or ST2 osteoblastic cells (23). This increase in  
6 RANKL from tumour cells and osteoblasts have the potential to stimulate osteoclastogenesis  
7 and drive the formation of osteolytic lesions. Disrupting this interaction via administration of  
8 pharmacological RANKL inhibitors including such as RANKL-Fc and OPG-Fc have been show  
9 to prevent tumour-associated bone destruction and reduce tumour growth in bone from a  
10 variety of tumours including breast, lung, prostate, renal and colon (reviewed in 24). In  
11 addition, giving OPG, either simultaneously with or before, tumour cell injection  
12 demonstrated that RANKL inhibition significantly delayed de novo formation of MDA-MB-  
13 231 breast cancer skeletal metastases (25). Pre-clinical studies show impressive anti-bone  
14 metastases effects with RANKL inhibitors and have led to the development of a fully human  
15 monoclonal antibody to RANKL (Denosumab) that is currently undergoing a number of  
16 clinical trials as a treatment for cancer induced bone disease and to increase bone  
17 metastasis-free survival (reviewed in 26 and 27). However, none of the pre-clinical studies  
18 have addressed the important clinical question of whether inhibiting RANKL has any effect  
19 on dormant tumour cells in the bone microenvironment.  
20  
21

22  
23  
24  
25  
26  
27  
28  
29  
30  
31 The majority of women who develop bone metastases are post-menopausal and recently  
32 published data from clinical trials have shown that treating patients at high risk of  
33 developing bone metastases with zoledronic acid is only beneficial to patients who are 5-  
34 years or more post-menopausal (28). These data indicate that inhibition of osteoclast  
35 activity may have specific anti-tumour effects in a low oestrogen environment. In the  
36 current study we mimic the post-menopausal low oestrogen environment by OVX. Our  
37 current data support our previous findings that OVX significantly increases osteoclast  
38 activity and stimulates proliferation of dormant disseminated tumour cells in bone (8). We now  
39 show that these processes are completely inhibited following weekly administration of  
40 25mg/kg OPG-Fc. *In vitro* co-culture studies with breast cancer (MDA-MB-231, MCF7 or  
41 T47D) cells and osteoblastic cells indicate that contact with bone can induce expression of  
42 RANKL by breast cancer cells and therefore it is possible that inhibiting RANKL may have  
43 direct anti-tumour effects on cancer cells growing in the skeleton (29). These findings may in  
44 part explain the increased survival benefit seen when treating breast and prostate cancer  
45 patients with bone metastases with denosumab compared with zoledronic acid (13).  
46  
47  
48  
49  
50  
51  
52  
53  
54  
55  
56  
57  
58  
59  
60

1  
2  
3 OPG-Fc is a pharmacologically enhanced native OPG synthesised by Amgen from which the  
4 heparin binding domain and the death domain homologous regions have been removed and  
5 the remaining amino acids 22-194 OPG peptide have been fused to the Fc domain of human  
6 IgG1 (15). The resulting OPG-Fc is a potent as full length OPG but shows a significantly  
7 increased circulating half-life. The compound we used is endotoxin free and has been used  
8 in multiple published *in vivo* studies (15, 30-36). The doses of OPG-Fc used in animal models  
9 of bone metastasis varied considerably depending on the cancer type and duration of the  
10 experiment (33-36). We chose to administer 25mg/kg OPG-Fc once per week, as this dose is  
11 previously shown to inhibit MDA-MB-231 tumour growth in bone. We confirmed that this  
12 treatment regime significantly decreased osteoclastic bone resorption in the mice, resulting  
13 in significantly decreased osteoclast and osteoblast activity and almost complete elimination  
14 of these cell types on the trabecular and endocortical surfaces of tibiae 4 weeks following  
15 commencement of treatment. Interestingly, despite decreased activity of osteoblasts, the  
16 growth tibial growth plates were significantly larger in OPG-Fc treated mice compared with  
17 control animals, a phenomenon also seen following administration of zoledronic acid (37).  
18 Safranin O staining revealed that the enlarged growth plates were made up of proteoglycan  
19 with increased numbers of chondrocytes, indicating that inhibition of osteoclast activity is  
20 modifying endochondral ossification in this model. However, as the primary goal of this  
21 study was to investigate the effects on inhibiting RANK-RANKL interactions on tumour  
22 growth in bone, the effects of OPG-Fc on chondrocytes will be the subject of separate  
23 investigations.

24  
25  
26  
27  
28  
29  
30  
31  
32  
33  
34  
35  
36  
37  
38 In conclusion, our study presents the first data showing that disruption of RANK-RANKL  
39 interactions following administration of OPG-Fc inhibits growth of dormant tumour cells  
40 disseminated in bone *in vivo*. Our data support early intervention with anti-resorptive  
41 therapy in a low-oestrogen environment to prevent development of bone metastases.  
42  
43  
44  
45  
46

#### 47 **Acknowledgments**

48  
49  
50 This study was supported by a program grant from Cancer Research UK (to CLE, PIC and IH).  
51 PIC is supported by Mrs Janice Gibson and the Ernest Heine Family Foundation. The IVIS  
52 Lumina II system was purchased with an equipment grant from Yorkshire Cancer Research.  
53 We are grateful for the support from Miss Orla Gallagher and Mr Darren Lath who provided  
54 expert bone processing and sectioning.  
55  
56  
57  
58  
59  
60

## References

1. Townson JL, Chambers AF. Dormancy of solitary metastatic cells. *Cell Cycle* 2006;**5**:1744-50.
2. Aguirre-Ghiso JA, Bragado P, Sosa MS. Metastasis awakening: targeting dormant cancer. *Nat Med* 2013;**19**:276-7.
3. Chen YC, Sosnoski DM, Mastro AM. Breast cancer metastasis to the bone: mechanisms of bone loss. *Breast Cancer Res* 2010;**12**:215.
4. Clézardin P. (2011) Therapeutic targets for bone metastases in breast cancer. *Breast Cancer Res*. 13(2):207.
5. Coleman RE, Rathbone E, Brown JE. Management of cancer treatment-induced bone loss. *Nat Rev Rheumatol* 2013;**9**:365-74.
6. Figueroa-Magalhães MC, Miller RS. Bone-modifying agents as adjuvant therapy for early-stage breast cancer. *Oncology (Williston Park)* 2012;**26**:955-62.
7. Coleman RE, Marshall H, Cameron D, Dodwell D, Burkinshaw R, Keane M, et al. Breast cancer adjuvant therapy with zoledronic acid. *N Engl J Med* 2011;**365**:1396-405
8. Ottewell PD, Wang N, Brown HK, Reeves KJ, Fowles CA, Croucher PI, Eaton CL, Holen I. Zoledronic Acid has differential antitumor activity in the pre- and postmenopausal bone microenvironment in vivo. *Clin Cancer Res* 2014;**20**:2922-32.
9. Ottewell PD, Wang N, Meek J, Fowles CA, Croucher PI, Eaton CL, Holen I. (2014) Castration-induced bone loss triggers growth of disseminated prostate cancer cells in bone. *End Rel Cancer* [EPUB ahead of print]



- 1  
2  
3  
4  
5  
6  
7  
8  
9  
10  
11  
12  
13  
14  
15  
16  
17  
18  
19  
20  
21  
22  
23  
24  
25  
26  
27  
28  
29  
30  
31  
32  
33  
34  
35  
36  
37  
38  
39  
40  
41  
42  
43  
44  
45  
46  
47  
48  
49  
50  
51  
52  
53  
54  
55  
56  
57  
58  
59  
60
10. Ottewell PD, Deux B, Monkkonon H, Cross SS, Coleman RE, Clezardin P and Holen I. Differential effect of doxorubicin and zoledronic acid on intraosseous versus extraosseous tumour growth in vivo. *Clin Can Res* 2008;**14**:4658-66.
11. van der Horst G, van den Hoogen C, Buijs JT, Cheung H, Bloys H, Pelger RC, Lorenzon G, Heckmann B, Feyen J, Pujuguet P, Blanque R, Clément-Lacroix P, van der Pluijm G. Targeting of  $\alpha(v)$ -integrins in stem/progenitor cells and supportive microenvironment impairs bone metastasis in human prostate cancer. *Neoplasia* 2011;**13**:516-25.
12. Zinonos I, Luo KW, Labrinidis A, Liapis V, Hay S, Panagopoulos V, Denichilo M, Ko CH, Yue GG, Lau CB, Ingman W, Ponomarev V, Atkins GJ, Findlay DM, Zannettino AC, Evdokiou A. Pharmacologic inhibition of bone resorption prevents cancer-induced osteolysis but enhances soft tissue metastasis in a mouse model of osteolytic breast cancer. *Int J Oncol* 2014;**45**:532-40.
13. Lipton A, Fizazi K, Stopeck AT, Henry DH, Brown JE, Yardley DA, Richardson GE, Siena S, Maroto P, Clemens M, Bilynskyy B, Charu V, Beuzeboc P, Rader M, Viniegra M, Saad F, Ke C, Braun A, Jun S. Superiority of denosumab to zoledronic acid for prevention of skeletal-related events: a combined analysis of 3 pivotal, randomised, phase 3 trials. *Eur J Cancer* 2012;**48**(16):3082-92.
14. Zauli G, Melloni E, Capitani S and Secchiero P. Role of full length osteoprotegerin in tumour cell biology. *Cell Mol Life Sci* 2009;**66**:841-815.
15. Morony S, Warmington K, Adamu S, Asuncion F, Geng Z, Grisanti M, Tan HL, Capparelli C, Starnes C, Weimann B, Dunstan CR, Kostenuik PJ. (2005) The inhibition of RANKL causes greater suppression of bone resorption and hypercalcemia compared with bisphosphonates in two models of humoral hypercalcemia of malignancy. *Endocrinology*. **146**(8):3235-43.
16. Ottewell PD, Monkkonen H, Jones M, Lefley DV Coleman RE and Holen I. (2008) Antitumour effects of doxorubicin followed by zoledronic acid in a mouse model of breast cancer. *J Natl Cancer Inst.* **100**:1167-78.

- 1  
2  
3  
4  
5  
6  
7  
8  
9  
10  
11  
12  
13  
14  
15  
16  
17  
18  
19  
20  
21  
22  
23  
24  
25  
26  
27  
28  
29  
30  
31  
32  
33  
34  
35  
36  
37  
38  
39  
40  
41  
42  
43  
44  
45  
46  
47  
48  
49  
50  
51  
52  
53  
54  
55  
56  
57  
58  
59  
60
17. Cole AA, Walters LM. Tartrate-resistant acid phosphatase in bone and cartilage following decalcification and cold embedding in plastic. (1987) *J Histochem Cytochem.* 35:203-6.
18. Mucowski SJ, Mack WJ, Shoupe D, Kono N, Paulson R, Hodis HN. (2014) Effect of prior oophorectomy on changes in bone mineral density and carotid artery intima-media thickness in postmenopausal women. *Fertil Steril.* 101(4):1117-22.
19. Liu XL, Li CL, Lu WW, Cai WX, Zheng LW. (2014) Skeletal site-specific response to ovariectomy in a rat model: change in bone density and microarchitecture. *Clin Oral Implants Res.* [EPUB ahead of print]
20. Lee SK, Kadono Y, Okada F, Jacquin C, Koczon-Jaremko B, Gronowicz G, Adams DJ, Aguila HL, Choi Y, Lorenzo JA. (2006) T lymphocyte-deficient mice lose trabecular bone mass with ovariectomy. *J Bone Miner Res.* 21(11):1704-12.
21. Bellahcene A, Bachelier R, Detry C, Lidereau R, Clezardin P, Castronovo V. (2007) Transcriptome analysis reveals an osteoblast-like phenotype for human osteotropic breast cancer cells. *Breast Cancer Research and Treatment.* 101:135-148
22. Zhao H, Ning LL, Wang ZY, Li HT, Qiao D, Yao Y, Qin HL. (2014) Calcitonin Gene-Related Peptide Inhibits Osteolytic Factors Induced by Osteoblast In Co-Culture System with Breast Cancer. *Cell Biochem Biophys.* [Epub ahead of print]
23. Park HR1, Min SK, Cho HD, Kim DH, Shin HS, Park YE. (2003) Expression of osteoprotegerin and RANK ligand in breast cancer bone metastasis. *J Korean Med Sci.* 18(4):541-6.
24. Roodman GD, Dougall WC. (2008) RANK ligand as a therapeutic target for bone metastases and multiple myeloma. *Cancer Treat Rev.* 34(1):92-101.
25. Canon JR, Roudier M, Bryant R, Morony S, Stolina M, Kostenuik PJ, Dougall WC. (2008) Inhibition of RANKL blocks skeletal tumor progression and improves survival in a mouse model of breast cancer bone metastasis. *Clin Exp Metastasis.* 25(2):119-29.

- 1  
2  
3  
4  
5  
6  
7  
8  
9  
10  
11  
12  
13  
14  
15  
16  
17  
18  
19  
20  
21  
22  
23  
24  
25  
26  
27  
28  
29  
30  
31  
32  
33  
34  
35  
36  
37  
38  
39  
40  
41  
42  
43  
44  
45  
46  
47  
48  
49  
50  
51  
52  
53  
54  
55  
56  
57  
58  
59  
60
26. Body JJ. (2013) Inhibition of RANK ligand to treat bone metastases. *Bull Cancer*. 100(11):1207-13.
27. Casas A, Llombart A, Martín M. (2013) Denosumab for the treatment of bone metastases in advanced breast cancer. *Breast*. 22(5):585-92.
28. Gnant M, Mlineritsch B, Stoeger H, Luschin-Ebengreuth G, Heck D, Menzel C, Jakesz R, Seifert M, Hubalek M, Pristauz G, Bauernhofer T, Eidtmann H, Eiermann W, Steger G, Kwasny W, Dubsy P, Hochreiner G, Forsthuber EP, Fesl C, Greil R; Austrian Breast and Colorectal Cancer Study Group, Vienna, Austria. (2011) Adjuvant endocrine therapy plus zoledronic acid in premenopausal women with early-stage breast cancer: 62-month follow-up from the ABCSG-12 randomised trial. *Lancet Oncol*. 12(7):631-41
29. Thomas RJ, Guise TA, Yin JJ, Elliott J, Horwood NJ, Martin TJ, Gillespie MT. (1999) Breast cancer cells interact with osteoblasts to support osteoclast formation. *Endocrinology*. 140(10):4451-8.
30. Miller RE, Jones JC, Tometsko M, Blake ML, Dougall WC. (2014) RANKL inhibition blocks osteolytic lesions and reduces skeletal tumor burden in models of non-small-cell lung cancer bone metastases. *J Thorac Oncol*. 9(3):345-54.
31. Canon J, Bryant R, Roudier M, Branstetter DG, Dougall WC. (2012) RANKL inhibition combined with tamoxifen treatment increases anti-tumor efficacy and prevents tumor-induced bone destruction in an estrogen receptor-positive breast cancer bone metastasis model. *Breast Cancer Res Treat*. 135(3):771-80.
32. Canon J, Bryant R, Roudier M, Osgood T, Jones J, Miller R, Coxon A, Radinsky R, Dougall WC. (2010) Inhibition of RANKL increases the anti-tumor effect of the EGFR inhibitor panitumumab in a murine model of bone metastasis. *Bone*. 46(6):1613-9.
33. Zauli G, Melloni E, Capitani S, Secchiero P. (2009) Role of full-length osteoprotegerin in tumor cell biology. *Cell Mol Life Sci*. 66(5):841-51.

1  
2  
3 34. Armstrong AP, Miller RE, Jones JC, Zhang J, Keller ET, Dougall WC. (2008) RANKL acts  
4 directly on RANK-expressing prostate tumor cells and mediates migration and expression of  
5 tumor metastasis genes. *Prostate*. 68(1):92-104.  
6  
7

8  
9 35. Vanderkerken K, De Leenheer E, Shipman C, Asosingh K, Willems A, Van Camp B,  
10 Croucher P. (2003) Recombinant osteoprotegerin decreases tumor burden and increases  
11 survival in a murine model of multiple myeloma. *Cancer Res*. 63(2):287-9.  
12  
13

14  
15 36. Morony S, Capparelli C, Sarosi I, Lacey DL, Dunstan CR, Kostenuik PJ. (2001)  
16 Osteoprotegerin inhibits osteolysis and decreases skeletal tumor burden in syngeneic and  
17 nude mouse models of experimental bone metastasis. *Cancer Res*. 61(11):4432-6.  
18  
19

20  
21 37. Haider M-T, Holen I, Hunter K, Brown HK (2014) Modifying the osteoblastic niche  
22 with zoledronic acid in vivo - potential implications for breast cancer bone metastasis *Bone*.  
23 66:240-50  
24  
25  
26

#### 27 28 **Figure legends**

29  
30 **Figure 1. Effects of ovariectomy on proliferation of MDA-MB-231 breast cancer cells in**  
31 **bone following long-term dormancy.** Panel a) is a diagrammatic representation of the  
32 protocol. Panel b) presents photographs of luciferase expressing MDA-MB-231 cells growing  
33 in female BALB/c nude mice 84 days following tumour cell injection and 28 days following  
34 ovariectomy or sham operation. Percentage of mice with tumours growing in bone and soft  
35 tissue **on day 56 (at ovariectomy)** and after ovariectomy are show in in panel c. Panel d  
36 shows dormant MDA-MB-231 cells in mouse tibia 56 days after tumour cell injection and  
37 panel e shows the effect of ovariectomy on bone volume 28 days following operation.  
38  
39  
40  
41  
42  
43  
44  
45

46  
47 **Figure 2. Effects of OPG-Fc on mouse long bone.** Female BALB/c nude mice were treated  
48 with 25mg/kg OPG-Fc or 0.1ml of 0.2% saline 1x per week for 4 weeks, panel a) shows  
49 histological sections following Goldner's staining (bone shown in green), Safranin O staining  
50 (non-ossified bone shown in red) and TRAP staining (osteoclasts can be identified as large,  
51 pink, multinucleated cells lining the bone surface and osteoblasts are highlighted with black  
52 arrows).  $\mu$ CT images showing bone architecture are shown in panel b) and panel c) is a graph  
53 showing the effects of OPG-Fc on bone volume compared with trabecular volume  $\pm$  SEM.  
54  
55  
56  
57  
58  
59  
60

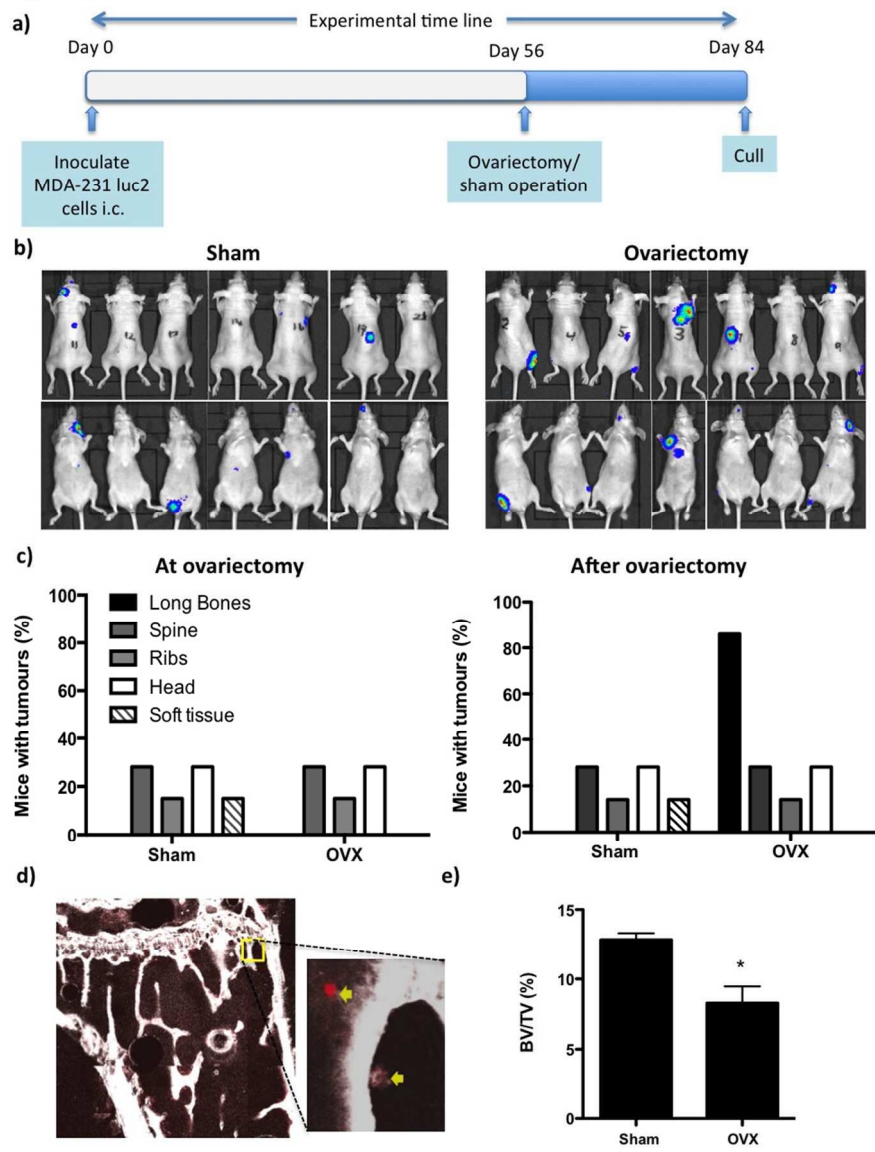
1  
2  
3 ELISA analysis of serum TRAP (units per litre) and P1NP (ng/ml)  $\pm$  SEM are shown in panels d)  
4 and e) respectively. \* =  $p < 0.01$ , \*\*\* =  $p < 0.0001$ .  
5  
6

7 **Figure 3. Effects of OPG-Fc on growth of MDA-MB-231 tumour cells *in vitro*.** Line graphs  
8 showing effects of increasing concentration of OPG-Fc on growth of MDA-MB-231 tumour  
9 cells in media supplemented with 10% FCS a) and reduced serum concentration on growth  
10 of MDA-MB-231 tumour cells treated with saline or 100g/ml OPG-Fc b) for up to 6 days in  
11 culture. Panel c) shows effects of increasing concentrations of OPG-Fc on ability of MDA-MB-  
12 231 cells to form colonies on plastic. Data presented as mean  $\pm$  SEM.  
13  
14  
15  
16

17  
18  
19  
20 **Figure 4. Effects of OPG-Fc on ovariectomy-induced tumour growth in bone.** Panel a) is a  
21 diagrammatic representation of the experimental protocol. Panel b) presents photographs  
22 of luciferase expressing MDA-MB-231 cells growing in female BALB/c nude mice 31 days  
23 following injection of saline or OPG-Fc and 28 days following ovariectomy or sham operation.  
24 Panel c) shows the percentage of mice with tumours in bone and outside of bone (lungs and  
25 eye socket) at the end of the experiment and panel d) shows mean bioluminescence per  
26 tumour in bone and outside of bone  $\pm$  SEM. \*\*\* =  $p < 0.0001$ . Panel e) shows  
27 photomicrographs of H&E stained histological sections from the left tibiae of BALB/c nude  
28 mice 31 day following injection of saline or OPG-Fc and 28 days following ovariectomy or  
29 sham operation, tumour circumference in bone is highlighted in blue.  
30  
31  
32  
33  
34  
35  
36

37 **Figure 5. Effects of OPG-Fc on ovariectomy-induced bone loss in the tibia.** Panel a) shows  
38 cross sectional and longitudinal images of female BALB/c mouse tibiae following 4 weekly  
39 injections of saline (control) or 25mg/kg OPG-Fc and 28 days following either sham  
40 operation or ovariectomy. Panel b) shows trabecular volume compared with bone volume  
41 for these mice and panels c) and d) show ELISA analysis of serum TRAP (units per litre) and  
42 P1NP (ng/ml)  $\pm$  SEM respectively. \*\*\* =  $P < 0.0001$   
43  
44  
45  
46  
47  
48  
49  
50  
51  
52  
53  
54  
55  
56  
57  
58  
59  
60

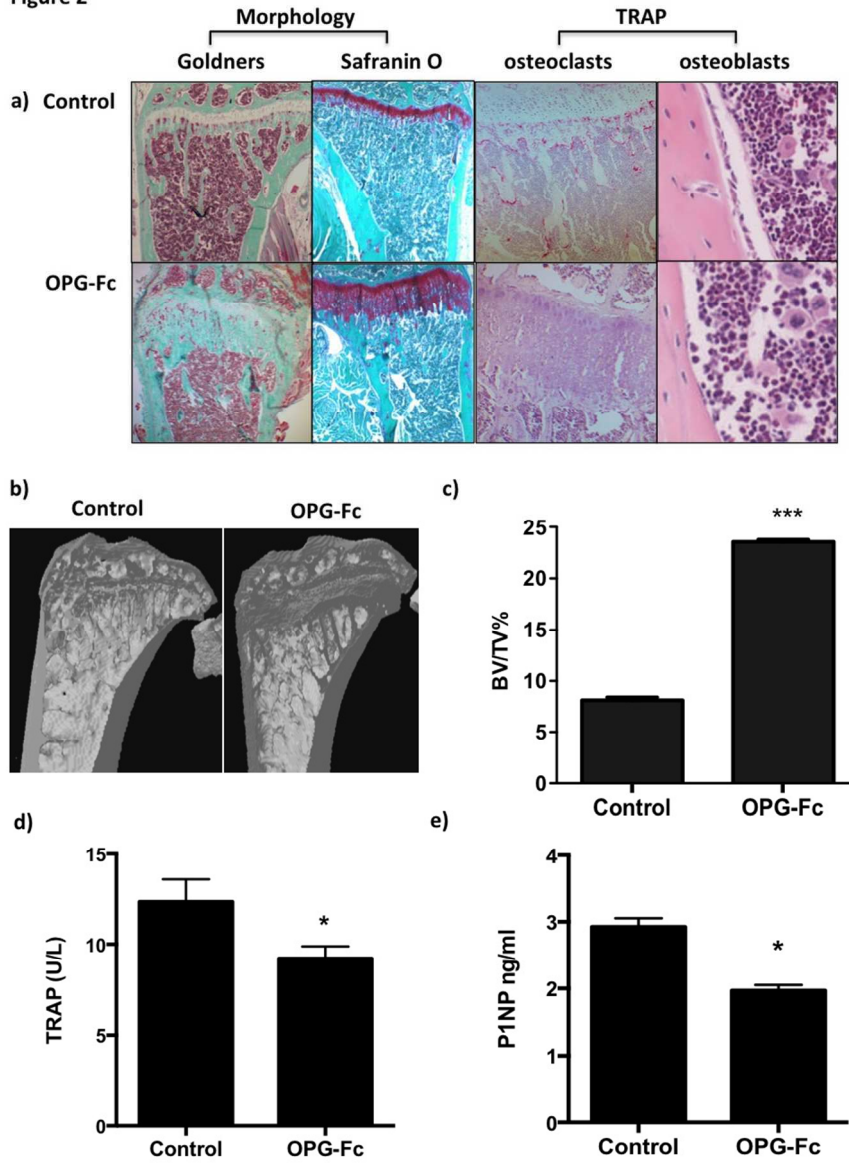
Figure 1



352x470mm (72 x 72 DPI)

1  
2  
3  
4  
5  
6  
7  
8  
9  
10  
11  
12  
13  
14  
15  
16  
17  
18  
19  
20  
21  
22  
23  
24  
25  
26  
27  
28  
29  
30  
31  
32  
33  
34  
35  
36  
37  
38  
39  
40  
41  
42  
43  
44  
45  
46  
47  
48  
49  
50  
51  
52  
53  
54  
55  
56  
57  
58  
59  
60

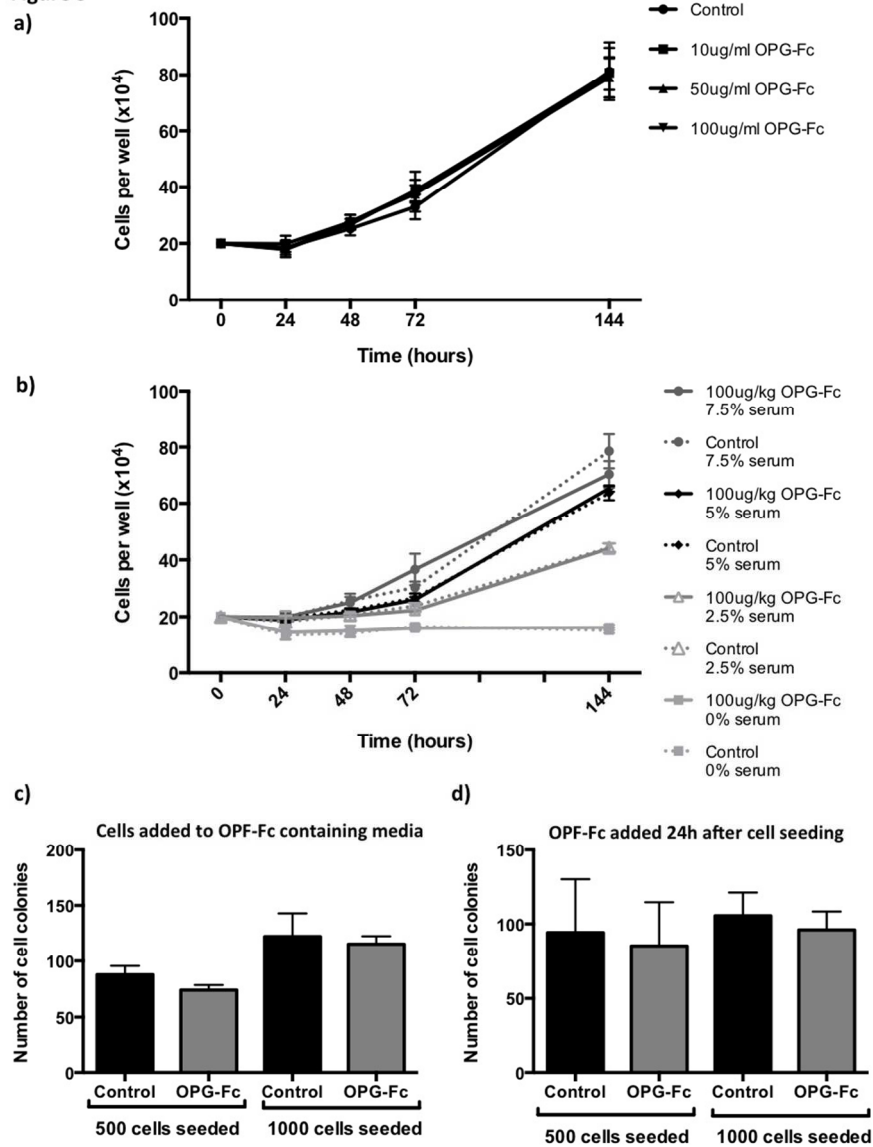
Figure 2



352x470mm (72 x 72 DPI)

1  
2  
3  
4  
5  
6  
7  
8  
9  
10  
11  
12  
13  
14  
15  
16  
17  
18  
19  
20  
21  
22  
23  
24  
25  
26  
27  
28  
29  
30  
31  
32  
33  
34  
35  
36  
37  
38  
39  
40  
41  
42  
43  
44  
45  
46  
47  
48  
49  
50  
51  
52  
53  
54  
55  
56  
57  
58  
59  
60

Figure 3

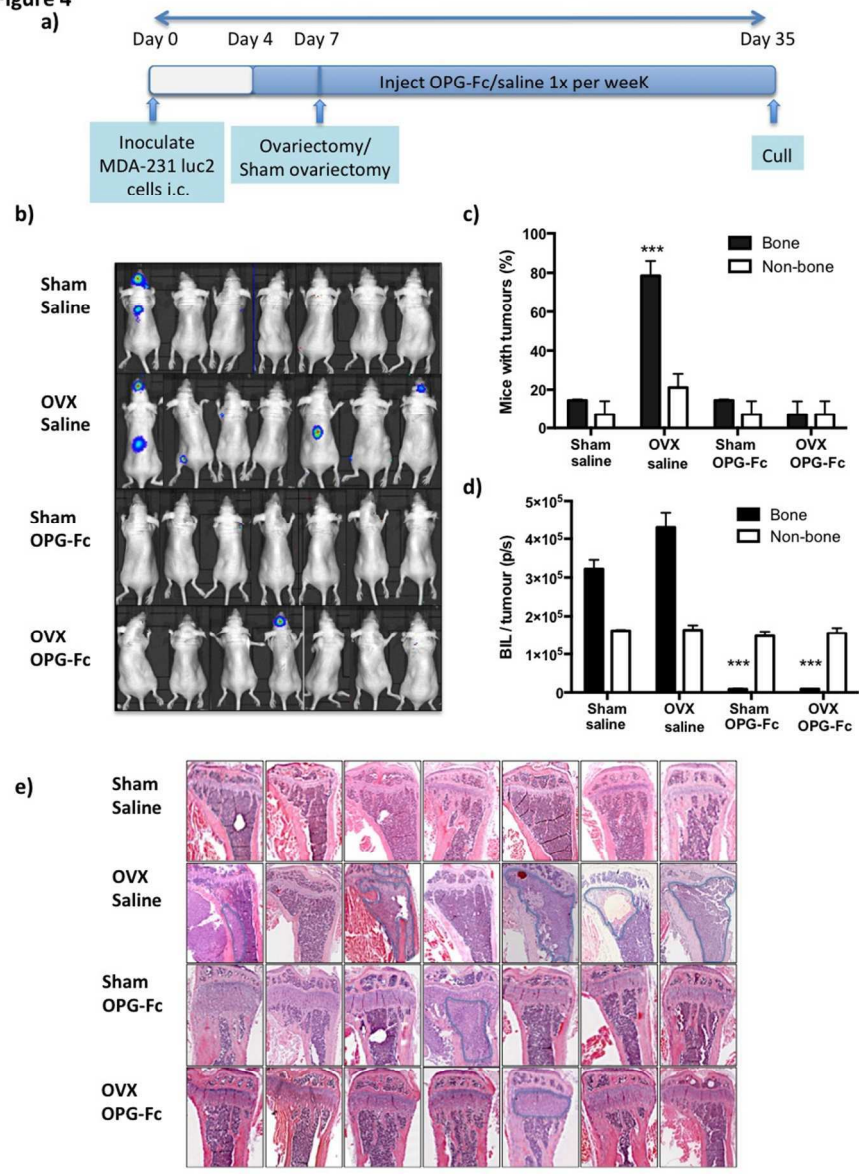


352x470mm (72 x 72 DPI)



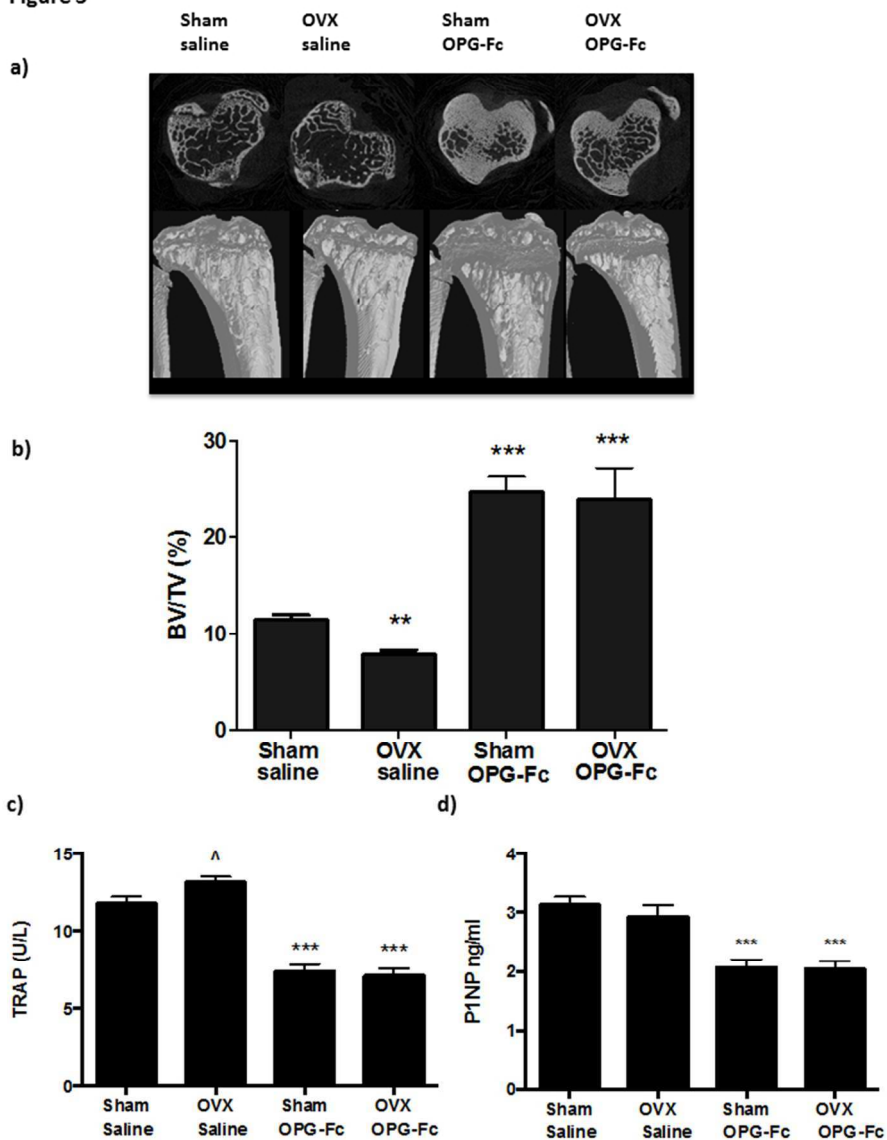
1  
2  
3  
4  
5  
6  
7  
8  
9  
10  
11  
12  
13  
14  
15  
16  
17  
18  
19  
20  
21  
22  
23  
24  
25  
26  
27  
28  
29  
30  
31  
32  
33  
34  
35  
36  
37  
38  
39  
40  
41  
42  
43  
44  
45  
46  
47  
48  
49  
50  
51  
52  
53  
54  
55  
56  
57  
58  
59  
60

Figure 4



352x470mm (72 x 72 DPI)

Figure 5



190x254mm (96 x 96 DPI)

1  
2  
3  
4  
5  
6  
7  
8  
9  
10  
11  
12  
13  
14  
15  
16  
17  
18  
19  
20  
21  
22  
23  
24  
25  
26  
27  
28  
29  
30  
31  
32  
33  
34  
35  
36  
37  
38  
39  
40  
41  
42  
43  
44  
45  
46  
47  
48  
49  
50  
51  
52  
53  
54  
55  
56  
57  
58  
59  
60